

High-energy phosphotransfer in the failing mouse heart: role of adenylate kinase and glycolytic enzymes

Dunja Aksentijević¹, Craig A. Lygate¹, Kimmo Mäkinen¹, Sevasti Zervou¹, Liam Sebag-Montefiore¹, Debra Medway¹, Hannah Barnes^{1,2}, Jurgen E. Schneider^{1,2}, and Stefan Neubauer^{1*}

¹Department of Cardiovascular Medicine, Wellcome Trust Centre for Human Genetics, University of Oxford, Roosevelt Drive, Oxford OX3 7BN, UK; and ²British Heart Foundation Experimental Magnetic Resonance Unit, Wellcome Trust Centre for Human Genetics, University of Oxford, Roosevelt Drive, Oxford, OX3 7BN, UK

Received 30 April 2010; revised 14 July 2010; accepted 30 July 2010; online publish-ahead-of-print 12 October 2010

See page 1268 for the editorial comment on this article (doi:10.1093/eurjhf/hfq193)

Aims

To measure the activity of the key phosphotransfer enzymes creatine kinase (CK), adenylate kinase (AK), and glycolytic enzymes in two common mouse models of chronic heart failure.

Methods and results

C57BL/6 mice were subjected to transverse aortic constriction (TAC), myocardial infarction induced by coronary artery ligation (CAL), or sham operation. Activities of phosphotransfer enzymes CK, AK, glyceraldehyde-3-phosphate dehydrogenase (GAPDH), 3-phosphoglycerate kinase (PGK), and pyruvate kinase were assessed spectrophotometrically. Mice were characterized by echocardiography or magnetic resonance imaging 5- to 8-week post-surgery and selected for the presence of congestive heart failure. All mice had severe left ventricular hypertrophy, impaired systolic function and pulmonary congestion compared with sham controls. A significant decrease in myocardial CK and maximal CK reaction velocity was observed in both experimental models of heart failure. However, the activity of AK and its isoforms remained unchanged, despite a reduction in its protein expression. In contrast, the activities of glycolytic phosphotransfer mediators GAPDH and PGK were 19 and 12% higher in TAC, and 31 and 23% higher in CAL models, respectively.

Conclusion

Chronic heart failure in the mouse is characterized by impaired CK function, unaltered AK, and increased activity of glycolytic phosphotransfer enzymes. This pattern of altered phosphotransfer activity was observed independent of the heart failure aetiology.

Keywords

Heart failure • Energy metabolism • Adenylate kinase • Creatine kinase • Phosphotransfer

Introduction

Intracellular phosphotransfer networks play a central role in myocardial energetics. Creatine kinase (CK)-catalysed high-energy phosphotransfer is the major pathway coupling cytosolic ATP demand to mitochondrial ATP production. Alterations in the components of the CK system, namely reduced creatine, phosphocreatine (PCr), and total CK, Mito-, MM-, and MB-CK isoenzymes activities are hallmarks of heart failure that are species- and model-independent.^{1–3} In addition, the importance of the CK system in heart failure is

underlined by the prognostic value of the PCr/ATP ratio, which is a stronger predictor of total and cardiovascular mortality than clinical functional status or left ventricular (LV) ejection fraction (EF).⁴ However, mice that are creatine-free due to knockout of a key enzyme in creatine biosynthesis (guanidinoacetate-*N*-methyltransferase) have a surprisingly mild cardiac phenotype,⁵ as do other transgenic ablation models such as Mito-CK and M-CK (CK double KO mice).⁶ Collectively, these studies indicate the potential for compensatory mechanisms to support contractile function in the energetically compromised heart.

* Corresponding author. Department of Cardiovascular Medicine, University of Oxford, John Radcliffe Hospital, Oxford OX3 9DU, UK. Tel: +44 1865 851 085, Fax: +44 1865 222 077, Email: stefan.neubauer@cardiov.ox.ac.uk

In addition to CK, adenylate kinase (AK) mediates a complementary intracellular phosphotransfer network.⁷ AK is a ubiquitous enzyme catalysing the reaction $2\text{ADP} \leftrightarrow \text{AMP} + \text{ATP}$. It promotes high-energy phosphoryl (P_i) transfer from mitochondria to ATP consumption sites via distinct isoforms with different cellular localizations.⁸ AK_1 is the major myocardial isoform localized in the cytosol near myofibrils, acting as a metabolic core by connecting: AK_2 , AK_3 (mitochondria membrane and matrix), AK_6 (nucleus), ecto-AK (extracellular space), and $\text{AK}_1\beta$ (plasma membrane).⁸

Although AK contribution to myocardial phosphotransfer is only $\sim 10\%$,⁹ in response to metabolic stress, AK facilitates transfer and utilization of an emergency energy reserve in the form of ATP- β and generates AMP, hence augmenting the small ATP/ADP changes into a much larger increase in the AMP:ATP ratio.^{7,10} This triggers a metabolic signalling cascade, resulting in increased ATP production via AMPK activation and hence regulating myocardial energy homeostasis.⁷

Furthermore, studies of AK and CK single and double knockouts have postulated a role for glycolytic enzyme phosphotransfer capacity as a potential compensatory mechanism.^{11,12} These studies suggest that linear arrays of glycolytic enzymes such as near equilibrium glyceraldehyde-3-phosphate dehydrogenase/3-phosphoglycerate kinase (GAPDH/PGK) enzymes have the ability to transfer high-energy phosphates, as well as generate additional ATP as a product of glycolysis.¹³ The mitochondrial high-energy phosphates traversing the glycolytic pathway can be used to phosphorylate ADP via the pyruvate kinase (PK)-catalysed reaction in the cytosol. Near equilibrium reactions catalysed by the GAPDH-PGK chain could also facilitate the transfer of P_i and NADH from the cytosol to mitochondria.⁷ Taken together, this suggests an auxiliary role for glycolytic intermediates, and the GAPDH/PGK shuttle in particular, in intracellular high-energy phosphate distribution.

Reports published to date regarding the role of AK and glycolytic phosphotransfers in heart failure are limited solely to the pacing-induced heart failure model in dogs. These studies showed increased AK-mediated phosphotransfer⁹ in contrast to decreased myocardial AK, PK, and PGK activities.¹⁴ However, the general applicability to other species or models of heart failure is unknown.

Consequently, the aim of this study was to examine the role of enzymes catalysing the supplementary intracellular phosphotransfer: AK_{total} , AK_1 , $\text{AK}_{\text{remnant}}$ and glycolytic enzymes PGK, GAPDH, and PK in two different murine models of heart failure.

Methods

All procedures were performed in accordance with the Home Office Guidance on the Operation of Animals (Scientific Procedures) Act 1986.

Transverse aortic constriction

C57BL/6J male mice (body weight 24 ± 3 g) were anaesthetized with isoflurane, intubated, and a transsternal thoracotomy performed [sham = 8, transverse aortic constriction (TAC) = 12]. The transverse aorta was constricted with a 7-0 polypropylene monofilament suture (Ethicon) tied against a 27 G needle or sham operation performed

as described by Lygate *et al.*¹⁵ All mice received an echocardiogram every 1–2 weeks and were taken off procedure when clear evidence for LV hypertrophy and heart failure was observed (mean follow-up was 5-week post-surgery). Owing to limited tissue availability, stock C57BL/6 male mice were used as controls for the hexokinase activity assay.

Coronary artery ligation

Myocardial infarction was induced by surgical ligation of the left anterior descending coronary artery or sham operation in adult female C57BL/6 mice [body weight 20 ± 3 g; sham = 15, coronary artery ligation (CAL) = 22] as described previously.¹⁶

At 6–8 weeks after infarction, mice received either a magnetic resonance imaging (MRI) or three-dimensional (3D) echocardiogram examination to assess cardiac structure and function, and a small subset of representative animals also received LV haemodynamic measurements (sham = 5, CAL = 3).

In vivo measurement of LV function

Heart failure was defined in both experimental groups based on the *in vivo* LV dysfunction (EF $> 2\text{SD}$ lower than sham), morphometric LV parameters (myocardial cross-section area $> 2\text{SD}$ greater than sham, LV weight $> 2\text{SD}$ greater than sham), and pulmonary congestion (post-mortem wet lung weight/body weight $> 2\text{SD}$ greater than sham).³ Only mice with lung weight/body weight $> 2\text{SD}$ than sham were used in this study.

Cine magnetic resonance imaging

Global cardiac functional parameters were assessed using cine MRI in a subset of CAL mice (sham = 4, CAL = 6) under isoflurane anaesthesia as described before.¹⁷ In brief, the mice were scanned in a horizontal bore 9.4 T MR system (Varian Inc., Palo Alto, CA, USA), equipped with a shielded gradient insert (1000 mT/m; rise time, 130 μs). A quadrature-driven birdcage coil (id 33 mm—Rapid Biomedical, Rimpar, Germany) was used to transmit/receive the magnetic resonance signals. Eight to nine contiguous slices were acquired in short-axis orientation covering the entire LV. The segmentation of the cine data was performed off-line using Amira 4.1 (Visage Imaging, Berlin, Germany) to measure LV volumes in end-diastole and end-systole, respectively.

Three-dimensional echocardiography

Three-dimensional echocardiography was performed under isoflurane anaesthesia (1–1.5%) using an Agilent Sonos 5500 with 6–15 MHz linear array transducer as described previously.³ Measurements were made from a single parasternal short-axis slice at the level of the papillary muscles (sham = 8, TAC = 12).

Left ventricular haemodynamics

A representative sample of mice fulfilling the above criteria was anaesthetized with isoflurane (1.25–1.5%) for the measurement of haemodynamic indices using a 1.4 F Millar Mikro-tip catheter (SPR-671) inserted into the LV via the carotid artery.¹⁸

Tissue harvest

All mice were euthanized by cervical dislocation, the heart excised, blotted, and weighed (in CAL mice, the infarct scar was then removed), before snap freezing in liquid nitrogen and storage at -80°C for biochemical analysis as described below.

Gene expression analysis

Quantitative reverse transcriptase–polymerase chain reaction (qRT–PCR) was used to detect mRNA levels of AK₁ which is the predominant AK isoform in the heart, contributing >70% of total intracellular AK activity.¹⁹ Total RNA was extracted from snap-frozen heart tissue of infarcted ($n = 4$) and sham ($n = 3$) in addition to banded ($n = 4$) and sham ($n = 3$) mice using the RNeasy Fibrous Tissue Kit (Qiagen, UK) as described previously.²⁰ Five nanograms of total RNA were used for RT prior to amplification reactions performed using Qiagen Quantitect SYBR Green RT–PCR kit (Qiagen) on the Rotor-Gene system (Corbett Research Ltd, UK). The relative quantities of endogenous AK₁ mRNA levels were normalized against the reference gene 36B4, using the following mouse oligonucleotide primers: 36B4 5'-AGATTCGGGATATGCTGTTGG-3'; reverse 5'-TCGGGTCCTA GACCAGTGTTC-3'; AK₁ forward 5'-CCAATGGCTTCCTGATCG A-3'; AK₁ reverse 5'-GCAAGTGTGGGCTGTCCAAT-3'. For data analysis, the double-standard curve method was employed, in which standard curves spanning five log dilutions of heart RNA were constructed for both the 36B4 and AK₁ primers.

Western blotting

SDS–PAGE and western blotting were used for the detection of the total protein expression of AK₁. Approximately 10 mg of frozen, grounded LV tissue was mixed with 500 μ L of extraction buffer: 50 mM Tris, 150 mM NaCl, 2% SDS, 1 mM DTT, 1 mM PMSF, and 1 pellet of protease inhibitor cocktail (Roche, UK) per 100 mL, and homogenized in a glass tissue homogenizer for 30 s, followed by 1 h incubation at 4°C with constant agitation. The extract was centrifuged at 10 000 g for 10 min at 4°C and the supernatant analysed for protein concentration using the BCA protein assay (Pierce, UK). Equal amounts of protein (40 μ g) were loaded onto SDS–PAGE gels (4% stacking gel and 12% separating gel) which were run at –200 V for 1 h followed by transfer onto a PVDF membrane (GE Healthcare, UK) at 200 mA overnight at 4°C. The membrane was stained with rabbit anti-AK₁ (Santa Cruz, UK), followed by goat anti-rabbit-HRP (Santa Cruz). To confirm equal loading of protein, the membrane was stripped of antibodies by incubating for 30 min in stripping buffer (2% SDS, 62.5 mM Tris–HCl, pH 6.8, and 100 mM 2-mercaptoethanol) at 55°C, followed by staining with mouse anti-mouse α -actinin (Sigma-Aldrich, UK) and goat anti-mouse-HRP (Promega, UK). The antibodies were detected with the ECL Advance chemiluminescence kit (GE Healthcare, UK) and the FluorChem 8800 imager.

Biochemical analysis

All chemicals, unless otherwise specified, were from Sigma-Aldrich (Poole, UK). Total creatine content was measured by HPLC as described previously.¹⁸ To calculate the intracellular creatine concentration, we assumed total heart protein content to be 0.17 g protein/g wet weight and intracellular volume 0.5 mL/g wet weight. The product of total myocardial creatine concentration and total CK activity was used as an estimate of *in vivo* maximal CK reaction velocity as described by Tian *et al.*²¹

The myocardial enzymatic activities of AK (AK_{total}, isoforms AK₁, and AK_{remnant}), and the glycolytic enzymes involved in high-energy phosphotransfer GAPDH, PGK, PK, and hexokinase were measured using coupled enzyme assays.¹⁴ Frozen, ground heart tissue (1 mg/mL) was extracted with the buffer containing 150 mM NaCl, 60 mM Tris–HCl, 5 mM EDTA, 0.2% Triton X-100, and mini-protease inhibitor (Roche), pH 7.5, for AK, PK, and PGK assays. For the GAPDH assay, heart tissue was lysed in a buffer containing 100 mM Tris–HCl

(pH 7.6), 10 mM glutathione reduced, and 1 mM EDTA extraction buffer. For the hexokinase assay, LV tissue was homogenized in a solution containing 150 mM KCl, 5 mM MgCl₂, 5 mM EDTA, and 5 mM 2-mercaptoethanol. The AK activity was recorded at 30°C, 340 nm in the assay buffer containing 100 mM potassium acetate (pH 7.5), 20 mM HEPES, 20 mM glucose, 4 mM MgCl₂, 2 mM NADP⁺, 1 mM EDTA, 1 mM dithiothreitol, 9 U/mL hexokinase, 4 U/mL glucose-6-phosphate dehydrogenase, and 2 mM ADP. The specific activity of AK₁ isoform was recorded by selective inhibition with 5 mM 5,5'-dithiobis(2-nitrobenzoic acid).²² The activity of the remaining myocardial AK isoforms was calculated as the difference between total AK activity and the activity of AK₁ and termed AK_{remnant}.²³ The PK activity was assayed at 30°C, 340 nm in media containing 50 mM imidazole (pH 7.6), 20 mM KCl, 2 mM MgCl₂, 0.1 mM EDTA, 0.1 mM NADH, 1 mM ADP, 4.5 U/mL lactate dehydrogenase, and 1 mM phosphoenolpyruvate. The activity of GAPDH was measured at 25°C, 340 nm using reaction mixture containing 100 mM Tris–HCl (pH 8.6), 5 mM sodium arsenate, 3 mM dithiothreitol, 1.5 mM NAD⁺, and 1.5 mM glyceraldehydes-3-phosphate. The PGK activity was recorded at 25°C, 340 nm in the assay medium containing 50 mM imidazole buffer (pH 7.6), 2 mM MgCl₂, 0.1 mM EDTA, 1 mM ATP, 5 mM 3-phosphoglycerate, and 0.2 mM NADH. The hexokinase activity was quantified at 30°C, 340 nm in the reaction mixture containing 47 mM Tris (pH 7.4), 10 mM MgCl₂, 0.8 mM NADP, 5 mM ATP (pH 7.0), 0.5 mM glucose, 0.27 mM 6-phosphogluconate, 5 mM 2-mercaptoethanol, and 2.5 U/mL glucose 6-phosphate dehydrogenase. The contaminating 6-phosphogluconate dehydrogenase activity was quantified simultaneously with the same assay reaction content except that no ATP, glucose, or glucose 6-phosphate dehydrogenase was present.

Statistics

All data are expressed as mean \pm standard deviation (SD). Statistical analysis was performed comparing TAC or CAL group with sham mice using unpaired Student's *t*-test.

Pearson's correlation coefficient was used to assess the relationship between the variables. Statistical analysis was carried out using SPSS statistics software v.16.0. Differences were considered significant when $P < 0.05$.

Results

Transverse aortic constriction

Five weeks after TAC, mice were characterized by significant and severe LV hypertrophy compared with shams (LV weight 172% of sham) and oedematous lungs indicative of pulmonary congestion secondary to chronic heart failure (Table 1). Furthermore, the TAC experimental group was characterized by significant LV dilatation (increased end-diastolic area) vs. sham controls accompanied by the deteriorating systolic function (myocardial fractional area change: 33 vs. 59% sham).

Transverse aortic constriction mice also displayed the expected alterations in the CK phosphotransfer system components with a significant reduction in total CK activity (18%) (Figure 1) and reduced maximal CK reaction velocity (total CK activity \times total creatine) (sham 490.8 ± 102 vs. TAC 345.4 ± 69 , $P < 0.001$). Furthermore, there was a positive correlation between systolic function (EF) and the maximal CK reaction velocity ($r = 0.54$, $P < 0.05$). Despite clear evidence of heart failure, enzyme activities

Table 1 Morphological and functional characteristics of the transverse aortic constriction heart failure model

	Sham (n = 8)	TAC HF (n = 12)
Morphology		
Body weight (g)	29 ± 4	28 ± 3
Heart weight (mg)	134 ± 25	225 ± 43**
LV weight (mg)	93 ± 18	160 ± 25**
RV weight (mg)	24 ± 4	40 ± 10**
Lung weight (mg)	149 ± 15	283 ± 138**
Lung/body weight	5 ± 0.5	11 ± 5**
Creatine (nmol/mg protein)	69 ± 5	68 ± 7
3D echocardiography		
EDA (cm ²)	0.11 ± 0.03	0.16 ± 0.03**
ESA (cm ²)	0.05 ± 0.02	0.10 ± 0.04**
MyoCSA (cm ²)	0.11 ± 0.02	0.19 ± 0.02**
HR (b.p.m.)	500 ± 45	494 ± 54
Fractional area change (%)	59 ± 12	33 ± 14**

Data presented as mean ± SD. EDA, end-diastolic area; ESA, end-systolic area; MyoCSA, myocardial cross-section area; HR, heart rate.
***P* < 0.01 vs. sham controls.

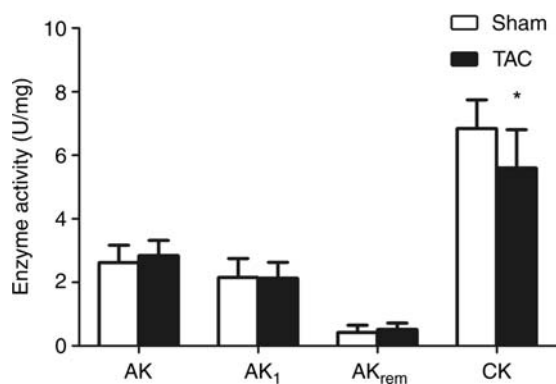


Figure 1 Adenylate kinase and creatine kinase activity in transverse aortic constriction heart failure. AK, total adenylate kinase; AK₁, AK 1 isoform; AK_{rem}, remnant AK isoforms (i.e. AK_{2,3,6}). Data presented as mean ± SD. Sham n = 8, transverse aortic constriction n = 12. **P* < 0.05 vs. sham controls.

of AK, AK₁, and the AK_{remnant} isoforms did not differ significantly between the two experimental groups (Figure 1). AK₁ mRNA levels remained unchanged (Figure 2) and the total protein expression of AK₁ was significantly reduced in TAC samples (50%) compared with sham (Figure 2).

The activity of hexokinase was not different between the two groups (Figure 3). In terms of the activities of glycolytic enzymes catalysing the high-energy P_i transfer, TAC mice were characterized by increased GAPDH and PGK and unaltered PK activity (Figure 3).

Furthermore, there was a significant negative correlation between total CK activity and GAPDH ($r = -0.624$ $P < 0.01$).

Coronary artery ligation

Six to eight weeks after CAL, a subset of animals received *in vivo* cine MRI and/or haemodynamic assessment, whereas all mice had post-mortem organ weight measurements (Table 2). CAL-induced heart failure was characterized by severe functional impairment and LV remodelling (Table 2). The LV was significantly dilated with the marked increase in the end-systolic and end-diastolic volumes (Table 2). Systolic function was severely impaired (EF 19 vs. 66% sham). There was an increase in wet lung weight confirming the presence of congestive heart failure.

As expected, total LV creatine content (Table 2) and total CK activity (Figure 4) were lower in the CAL heart failure group compared with sham controls. The maximal CK reaction velocity was significantly reduced in CAL heart failure (sham 374.8 ± 45 vs. CAL 260.3 ± 67 , $P < 0.05$). In agreement with the results in the TAC model, the AK_{total}, AK₁, and AK_{remnant} activities did not differ between the two experimental groups (Figure 4). The total AK₁ protein expression was significantly lower in the infarct group compared with sham (28% reduction, Figure 2); however, AK₁ mRNA levels remained unchanged (Figure 2). The activity of hexokinase did not differ significantly between the groups (Figure 5), whereas the changes in the glycolytic phosphotransfer enzymes were similar to the TAC model with significant increase in the activities of GAPDH and PGK in the CAL heart failure with no difference in the PK activity (Figure 5).

Furthermore, the analysis of the combined TAC and CAL enzymatic activity data revealed a significant negative correlation between PGK and total CK activities ($r = -0.511$ $P < 0.01$) (Figure 6) and between PGK and maximal CK activities ($r = -0.538$ $P < 0.01$).

Discussion

The major findings of this study are that the depressed CK-mediated phosphotransfer in the failing mouse hearts is accompanied by a concomitant increase in the activities of the glycolytic phosphotransfer catalysing enzymes GAPDH and PGK. However, the activity of AK, the main phosphotransfer enzyme supplementary to CK, was not altered. Clearly, the increase in the glycolytic phosphotransfer enzyme activity and preserved AK activity, while acting as a potentially compensatory mechanism, failed to maintain normal cardiac function in the failing hearts. Furthermore, this study shows that similar changes occur in two different surgical models of mouse heart failure, independently of the aetiology.

Studies in CK knockout mice suggest the presence of accessory enzymatic mechanisms, in the form of increased AK and glycolytic enzyme-catalysed phosphotransfer to support cellular energetics and contractile function.²⁴ However, despite a decrease in CK activity in both models of murine heart failure examined in this study, the activities of the components of the AK phosphotransfer system were unchanged. This observation is in contrast to the results from the canine pacing model of heart failure where a 30% decrease in CK was accompanied by a 21% decrease in the AK activity.¹⁴

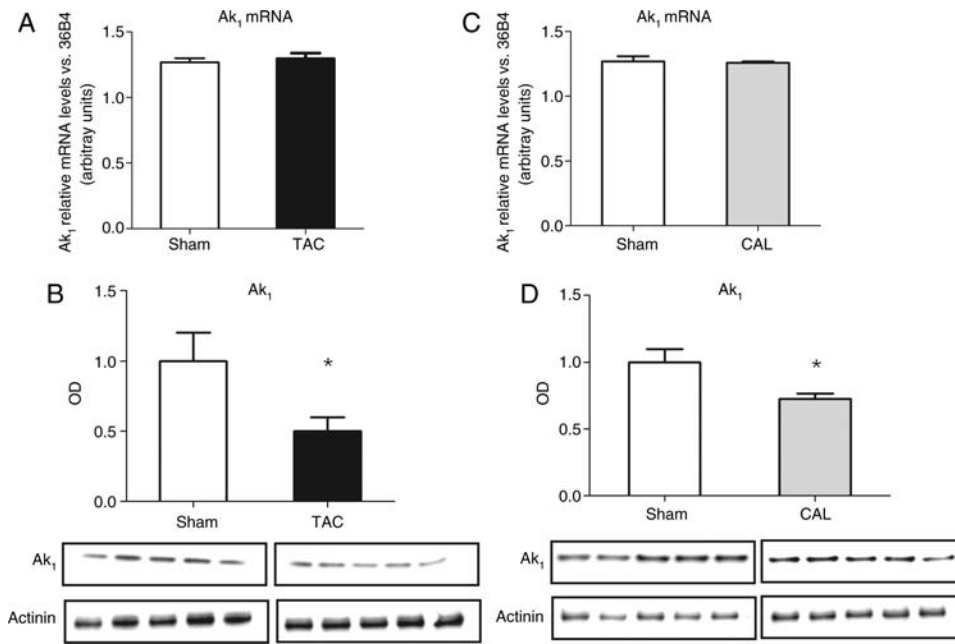


Figure 2 (A) AK₁ mRNA level in transverse aortic constriction heart failure, (B) AK₁ total protein expression in transverse aortic constriction heart failure, (C) AK₁ mRNA level in coronary artery ligation heart failure, and (D) AK₁ total protein expression in coronary artery ligation heart failure. mRNA levels are expressed in arbitrary units. Transverse aortic constriction sham $n = 3$, transverse aortic constriction $n = 4$, coronary artery ligation sham $n = 3$, coronary artery ligation $n = 4$. AK₁ optical density values are normalized against α -actinin and expressed as the relative change to the sham set as 1. The optical density values used for each experimental group are the average of three independent western blot experiments. Transverse aortic constriction sham $n = 6$, transverse aortic constriction $n = 7$, coronary artery ligation sham $n = 5$, coronary artery ligation $n = 5$. Data presented as mean \pm SD. * $P < 0.05$ vs. sham controls.

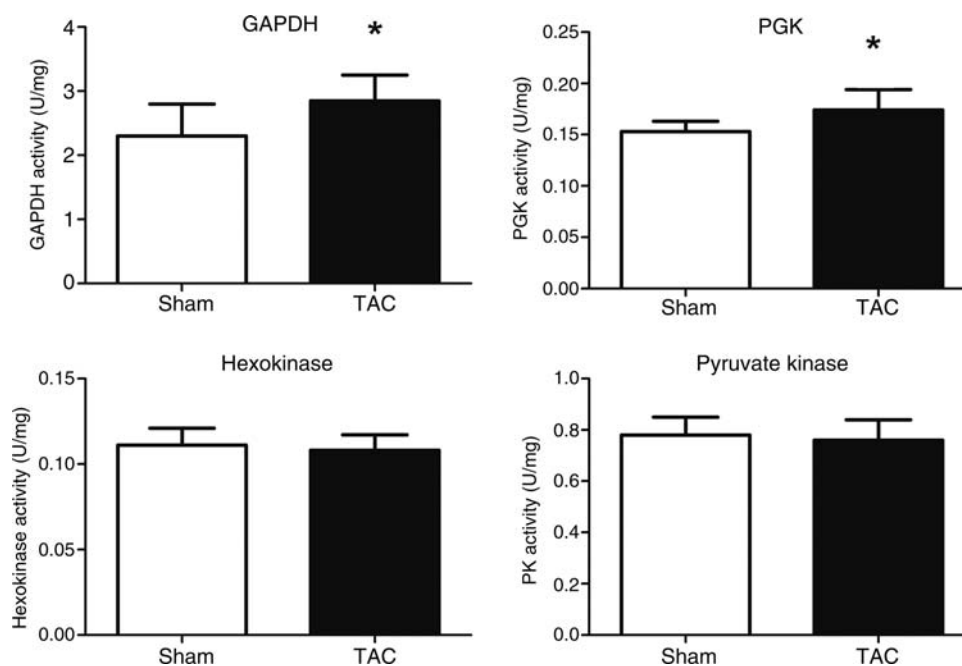


Figure 3 Glycolytic enzyme activities in transverse aortic constriction heart failure. GAPDH, PGK, and PK: sham $n = 8$, transverse aortic constriction $n = 12$; hexokinase $n = 4$. Data presented as mean \pm SD. * $P < 0.05$ vs. sham controls.

Table 2 Morphological and functional characteristics of the coronary artery ligation heart failure model

	Sham (n = 12)	CAL HF (n = 15)
Morphology		
Body weight (g)	24 ± 3	24 ± 2
Heart weight (mg)	115 ± 7	165 ± 18**
LV weight (mg)	78 ± 5	103 ± 10**
RV weight (mg)	21 ± 2	36 ± 10**
Lung weight (mg)	132 ± 8	199 ± 5**
Lung/body weight	5 ± 0.3	8 ± 3**
Creatine (nmol/mg protein)	66 ± 11	54 ± 10*
Infarct size (%)	—	47 ± 7
Cine MRI functional analysis	(n = 4)	(n = 6)
HR (b.p.m.)	440 ± 65	437 ± 50
EDV (μL)	58 ± 7	169 ± 22**
ESV (μL)	20 ± 8	136 ± 22**
EF (%)	66 ± 10	19 ± 5**
SV(μL)	38 ± 5	33 ± 7*
CO (mL/min)	17 ± 3	13 ± 3*
Haemodynamics	(n = 5)	(n = 3)
LVSP (mmHg)	102 ± 8	88 ± 10**
LVEDP (mmHg)	8 ± 4	19 ± 6**
dP/dt _{max} (mmHg/s)	8631 ± 2150	4757 ± 952**
dP/dt _{min} (mmHg/s)	-6794 ± 2547	-3398 ± 932**
Tau Weiss (ms)	6.6 ± 2	17.5 ± 4**

Data presented as mean ± SD. HR, heart rate; EDV, end-diastolic volume; ESV, end-systolic volume; EF, ejection fraction; SV, systolic volume (SV = EDV - ESV); CO, cardiac output (CO = SV × HR); LVSP, left ventricular systolic pressure; LVEDP, left ventricular end-diastolic pressure.

*P < 0.05.

**P < 0.01 vs. sham controls.

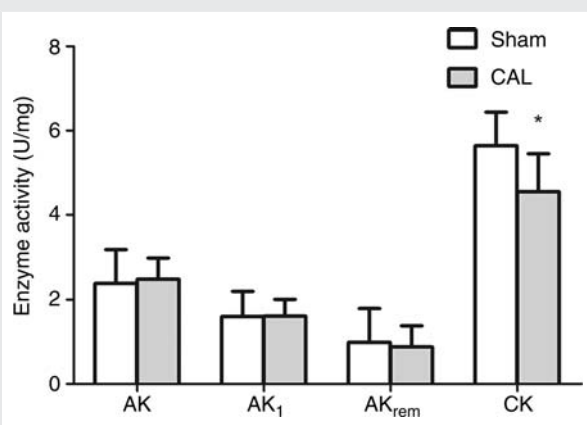


Figure 4 Adenylate kinase and creatine kinase activity in coronary artery ligation heart failure. AK, total adenylate kinase; AK₁, AK 1 isoform, AK_{rem}, remnant AK isoforms (i.e. AK_{2,3,6}). Sham n = 6–12, coronary artery ligation n = 13–14. Data presented as mean ± SD. *P < 0.05 vs. sham controls.

However, examination of the AK-mediated phosphotransfer dynamics in the same model of heart failure using [¹⁸O]-assisted ³¹P NMR revealed that AK-mediated phosphotransfer was actually increased, despite depressed AK and CK activities.⁹ Furthermore, it shows that the increase in AK-mediated phosphotransfer was only partially compensatory, as the sum of phosphotransfers mediated through CK and AK amounted to only ~65% of the total ATP turnover observed in healthy hearts. The deficit in enzyme-mediated phosphotransfer was provided by less efficient mechanisms such as simple diffusion and the glycolytic pathway.⁹ Therefore, unaltered AK activity in the face of compromised CK function in TAC and CAL models of murine heart failure may be interpreted as a compensatory mechanism since, as in the dog model, the relative contribution of AK to phosphotransfer is increased.

Surprisingly, the western blot analysis of total AK₁ protein expression in the LV samples indicated a significant reduction in total AK₁ protein expression in failing hearts, whereas AK₁ mRNA levels and enzyme activity remained unchanged. This pattern was observed in both models of heart failure. A mismatch between AK expression and activity was also observed in the canine model of heart failure, although in opposite direction, with no change in total AK expression, yet decreased enzyme activity and increased AK-mediated P_i flux.⁹ These discrepancies between gene expression, protein expression, and the activity suggest a complex interplay between AK protein expression and post-translational modification to influence AK-mediated phosphotransfer function in the failing heart. Additional experiments are required to determine the extent and nature of AK₁ post-translational modification, e.g. via phosphorylation, glycosylation, or oxidation, which are all characteristic of cardiac remodelling and failure.²⁵

Unaltered AK activity in TAC- and CAL-induced murine heart failure was accompanied by a compensatory increase in the GAPDH/PGK glycolytic enzyme activities. Skeletal muscles with chronic CK deficiency have been shown to shift a significant portion of the enzyme-catalysed phosphotransfer to the glycolytic mechanism,¹² and in our study, this is underlined by a significant negative correlation between maximal CK activity and GAPDH in the TAC heart failure model. In addition, if the glycolytic mechanism is also disabled in tissue deficient in CK (i.e. with the GAPDH inhibitor iodoacetamide), the compensation has been shown to shift to the AK-catalysed phosphoryl transfer.²⁶ We found that the activities of GAPDH and PGK were increased in both models of murine heart failure, which would be consistent with increased energetic contribution of near-equilibrium GAPDH/PGK-catalysed phosphotransfer. Increased activity of glycolytic enzymes may be due to loss of the direct inhibitory effect of PCr on the CK and glycolytic enzymatic rates through interdependence of AMP and ADP concentrations.²⁷ Furthermore, in addition to CK, PGK shuttle plays an important role in intracellular ADP removal,²⁸ and the negative correlation between PGK and CK (including maximal CK) activities (Figure 6) suggests a compensatory role of PGK in the intracellular adenine nucleotide ratio when the activity of CK is impaired in the failing heart.

Hexokinase is a glycolytic enzyme which is not thought to have significant involvement in intracellular phosphotransfer. It is bound

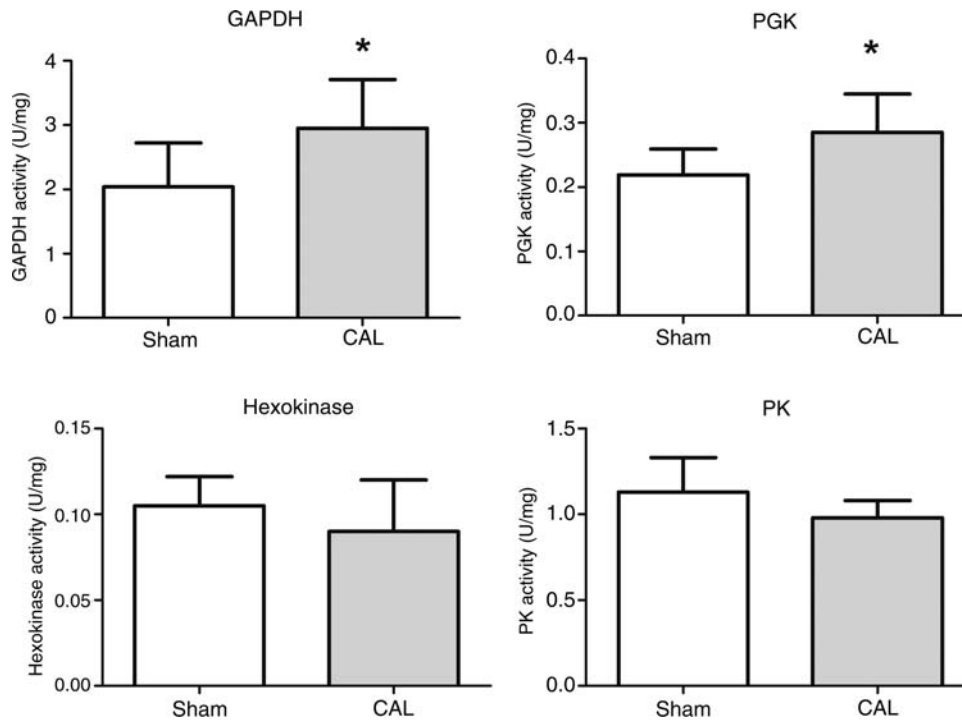


Figure 5 Glycolytic enzyme activities in coronary artery ligation heart failure. Sham $n = 7-9$, coronary artery ligation $n = 12-14$. Data presented as mean \pm SD. * $P < 0.05$ vs. sham controls.

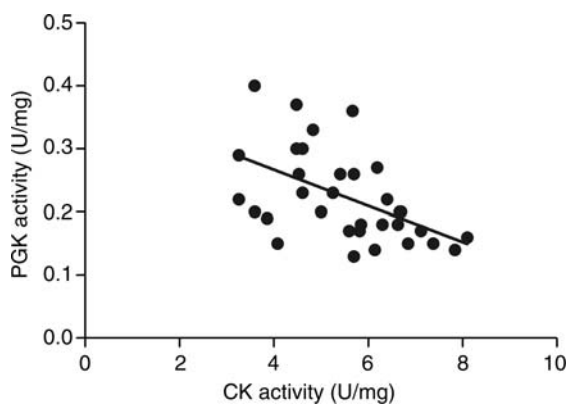


Figure 6 Relationship between creatine kinase and phosphoglycerate kinase activities in mice with congestive heart failure (transverse aortic constriction and coronary artery ligation) ($r = -0.511$ $P < 0.005$).

to the outer mitochondrial membrane and responsible for directing high-energy P_i from mitochondria into the glycolytic pathway. The unaltered hexokinase activity observed in both models of heart failure in this study is in agreement with the published observations in the canine pacing-induced heart failure¹⁴ and suggests that the increase in PGK and GAPDH enzyme activities is not due to a net increase in glycolysis. However, we cannot rule out that the changes in GAPDH and PGK activities play a

compensatory role by localizing glycolysis to bypass the need for effective phosphotransfer. For example, the direct delivery of glycolytic ATP to the SERCA pump has been described in CK- and MAK (M-CK/AK₁)-deficient mice.^{11,29} Regardless, from our study, it is evident that these increased activities are directionally the same in both experimental models, albeit smaller in comparison to those observed in large animal heart failure¹⁴ and humans,⁷ and most importantly insufficient to maintain normal cardiac function despite the unidirectional P_i exchange rate through GAPDH/PGK previously shown to approach values for oxidative phosphorylation and CK.³⁰

Study limitations

Owing to substantial technical difficulty in measuring the phosphotransfer in Langendorff-perfused CAL hearts, this study examines the total enzyme activities rather than phosphotransfer fluxes via specific enzymatic pathways. *In vitro* enzyme activities may exceed *in vivo* flux as the apparent excess in enzyme capacity is required to sustain phosphotransfer through multiple equilibrations at a rate corresponding to the functional requirement of the cardiac muscle.¹⁴ Nevertheless, the changes in enzyme activity measured here are likely to reflect a change in the flux capacity through specific metabolic pathway.

Conclusions

This is the first study of enzymes catalysing auxiliary high-energy phosphotransfer reactions in murine heart failure, namely AK

and glycolytic enzymes (GAPDH, PGK, and PK). In both models, severe functional impairment and extensive LV remodelling, commensurate with congestive heart failure, were accompanied by impairment in CK function.

An identical pattern of biochemical responses was observed, regardless of heart failure aetiology, with AK activity preserved, and increased activity of the glycolytic phosphotransfer mediators PGK and GAPDH, which may be compensatory. Our results support the concept of increased contribution to phosphotransfer by alternative non-CK pathways during cardiac failure. Further studies are required to determine whether augmentation of these pathways could provide a novel strategy to improve the energetic status of the failing heart.

Funding

This work was supported by the British Heart Foundation Programme Grant RG/05/005. We would also like to acknowledge Wellcome Trust Core Award Grant 075491/Z/04.

Conflict of interest: none declared.

References

1. Laser A, Ingwall JS, Tian R, Reis I, Hu K, Gaudron P, Ertl G, Neubauer S. Regional biochemical remodeling in non-infarcted tissue of rat heart post-myocardial infarction. *J Mol Cell Cardiol* 1996;**28**:1531–1538.
2. Neubauer S, Frank M, Hu K, Remkes H, Laser A, Horn M, Ertl G, Lohse MJ. Changes of creatine kinase gene expression in rat heart post-myocardial infarction. *J Mol Cell Cardiol* 1998;**30**:803–810.
3. Lygate CA, Fischer A, Sebag-Montefiore L, Wallis J, ten Hove M, Neubauer S. The creatine kinase energy transport system in the failing mouse heart. *J Mol Cell Cardiol* 2007;**42**:1129–1136.
4. Neubauer S, Horn M, Cramer M, Harre K, Newell JB, Peters W, Pabst T, Ertl G, Hahn D, Ingwall JS, Kochsiek K. Myocardial phosphocreatine-to-ATP ratio is a predictor of mortality in patients with dilated cardiomyopathy. *Circulation* 1997;**96**:2190–2196. ISSN: 0009-7322.
5. ten Hove M, Lygate CA, Fischer A, Schneider JE, Sang AE, Hulbert K, Sebag-Montefiore L, Watkins H, Clarke K, Isbrandt D, Wallis J, Neubauer S. Reduced inotropic reserve and increased susceptibility to cardiac ischemia/reperfusion injury in phosphocreatine-deficient guanidinoacetate-N-methyltransferase-knockout mice. *Circulation* 2005;**111**:2477–2485.
6. Saupe KW, Spindler M, Tian R, Ingwall JS. Impaired cardiac energetics in mice lacking muscle-specific isoenzymes of creatine kinase. *Circ Res* 1998;**82**:898–907.
7. Dzeja P, Chung S, Terzic A. Integration of adenylate kinase and glycolytic and glycogenolytic circuits in cellular energetics. In: Saks V, ed. *Molecular System Energetics: Energy for Life*. Weinheim: Wiley-VCH Verlag; 2007.
8. Dzeja P, Terzic A. Adenylate kinase and AMP signaling networks: metabolic monitoring, signal communication and body energy sensing. *Int J Mol Sci* 2009;**10**:1729–1772.
9. Dzeja PP, Vitkevicius KT, Redfield MM, Burnett JC, Terzic A. Adenylate kinase-catalyzed phosphotransfer in the myocardium: increased contribution in heart failure. *Circ Res* 1999;**84**:1137–1143.
10. Frederich M, Balschi JA. The relationship between AMP-activated protein kinase activity and AMP concentration in the isolated perfused rat heart. *J Biol Chem* 2002;**277**:1928–1932.
11. Janssen E, Terzic A, Wieringa B, Dzeja PP. Impaired intracellular energetic communication in muscles from creatine kinase and adenylate kinase (M-CK/AK1) double knock-out mice. *J Biol Chem* 2003;**278**:30441–30449.
12. de Groof AJ, Oerlemans FT, Jost CR, Wieringa B. Changes in glycolytic network and mitochondrial design in creatine kinase-deficient muscles. *Muscle Nerve* 2001;**24**:1188–1196.
13. Dzeja PP, Zeleznikar RJ, Goldberg ND. Adenylate kinase: kinetic behavior in intact cells indicates it is integral to multiple cellular processes. *Mol Cell Biochem* 1998;**184**:169–182.
14. Dzeja PP, Pucar D, Redfield MM, Burnett JC, Terzic A. Reduced activity of enzymes coupling ATP-generating with ATP-consuming processes in the failing myocardium. *Mol Cell Biochem* 1999;**201**:33–40.
15. Lygate CA, Schneider JE, Hulbert K, ten Hove M, Sebag-Montefiore LM, Cassidy PJ, Clarke K, Neubauer S. Serial high resolution 3D-MRI after aortic banding in mice: band internalization is a source of variability in the hypertrophic response. *Basic Res Cardiol* 2006;**101**:8–16.
16. Dawson D, Lygate CA, Saunders J, Schneider JE, Ye X, Hulbert K, Noble JA, Neubauer S. Quantitative 3-dimensional echocardiography for accurate and rapid cardiac phenotype characterization in mice. *Circulation* 2004;**110**:1632–1637.
17. Schneider JE, Cassidy PJ, Lygate C, Tyler DJ, Wiesmann F, Grieve SM, Hulbert K, Clarke K, Neubauer S. Fast, high-resolution *in vivo* cine magnetic resonance imaging in normal and failing mouse hearts on a vertical 11.7 T system. *J Magn Reson Imaging* 2003;**18**:691–701.
18. Ten Hove M, Chan S, Lygate C, Monfared M, Boehm E, Hulbert K, Watkins H, Clarke K, Neubauer S. Mechanisms of creatine depletion in chronically failing rat heart. *J Mol Cell Cardiol* 2005;**38**:309–313.
19. Pucar D, Bast P, Gumina RJ, Lim L, Drahl C, Juranic N, Macura S, Janssen E, Wieringa B, Terzic A, Dzeja PP. Adenylate kinase AK1 knockout heart: energetics and functional performance under ischemia-reperfusion. *Am J Physiol Heart Circ Physiol* 2002;**283**:H776–H782.
20. ten Hove M, Makinen K, Sebag-Montefiore L, Hunyor I, Fischer A, Wallis J, Isbrandt D, Lygate C, Neubauer S. Creatine uptake in mouse hearts with genetically altered creatine levels. *J Mol Cell Cardiol* 2008;**45**:453–459.
21. Tian R, Nascimben L, Kaddurah-Daouk R, Ingwall JS. Depletion of energy reserve via the creatine kinase reaction during the evolution of heart failure in cardiomyopathic hamsters. *J Mol Cell Cardiol* 1996;**28**:755–765.
22. Kress LF, Bono VH Jr, Noda L. The sulfhydryl groups of rabbit muscle adenosine triphosphate-adenosine monophosphate phosphotransferase. Activity of enzyme treated with mercurials. *J Biol Chem* 1966;**241**:2293–2300.
23. Vitkevicius KT, Dzeja P. Changes in adenylate kinase isoform activity in the ischemic rabbit heart. *Byulleten Experimental'noi Biologii i Meditsiny* 1990;**110**:148–149.
24. Dzeja PP, Zeleznikar RJ, Goldberg ND. Suppression of creatine kinase-catalyzed phosphotransfer results in increased phosphoryl transfer by adenylate kinase in intact skeletal muscle. *J Biol Chem* 1996;**271**:12847–12851.
25. McGregor E, Dunn MJ. Proteomics of heart disease. *Hum Mol Genet* 2003;**12**(Spec no. 2):R135–R144.
26. Dzeja PP, Terzic A, Wieringa B. Phosphotransfer dynamics in skeletal muscle from creatine kinase gene-deleted mice. *Mol Cell Biochem* 2004;**256–257**:13–27.
27. Kupriyanov VV, Seppet EK, Emelin IV, Saks VA. Phosphocreatine production coupled to the glycolytic reactions in the cytosol of cardiac cells. *Biochim Biophys Acta* 1980;**592**:197–210.
28. Dzeja PP, Terzic A. Phosphotransfer networks and cellular energetics. *J Exp Biol* 2003;**206**(Pt 12):2039–2047.
29. Boehm E, Ventura-Clapier R, Mateo P, Lechene P, Veksler V. Glycolysis supports calcium uptake by the sarcoplasmic reticulum in skinned ventricular fibres of mice deficient in mitochondrial and cytosolic creatine kinase. *J Mol Cell Cardiol* 2000;**32**:891–902.
30. Kingsley-Hickman PB, Sako EY, Mohanakrishnan P, Robitaille PM, From AH, Foker JE, Ugurbil K. 31P NMR studies of ATP synthesis and hydrolysis kinetics in the intact myocardium. *Biochemistry* 1987;**26**:7501–7510.